



# Optical dielectric function of Si(2,6-bis(benzimidazol-2'-yl)pyridine)<sub>2</sub> determined by spectroscopic ellipsometry

YANZENG LI,<sup>1,\*</sup>  MARGARET KOCHERGA,<sup>2</sup> SERANG PARK,<sup>1</sup> MARC LATA,<sup>1</sup> MICHEAL MCLAMB,<sup>1</sup> GLENN BOREMAN,<sup>1</sup> THOMAS A. SCHMEDAKE,<sup>2</sup> AND TINO HOFMANN<sup>1,3</sup>

<sup>1</sup>Department of Physics and Optical Science, University of North Carolina at Charlotte, 9201 University City Blvd., Charlotte, NC 28223, USA

<sup>2</sup>Department of Chemistry, University of North Carolina at Charlotte, 9201 University City Blvd., Charlotte, NC 28223, USA

<sup>3</sup>THz Materials Analysis Center, Department of Physics, Chemistry, and Biology (IFM), Linköping University, SE 581 83 Linköping, Sweden

\*yli91@uncc.edu

**Abstract:** Si(bzimpy)<sub>2</sub>, a fluorescent organic complex, has been demonstrated as a potential electron transport and electroluminescent layer for organic electronic devices. Despite the successful synthesis and encouraging electroluminescence at 560 nm, the complex dielectric function of the water-stable complex has not been reported yet. In this letter, we report on the first spectroscopic ellipsometry data obtained from a Si(bzimpy)<sub>2</sub> thin film in the spectral range from 300 nm to 1900 nm (0.65 eV to 4.1 eV). A parameterized model dielectric function composed of a Tauc-Lorentz and Gaussian oscillators is employed to analyze the experimental ellipsometry data. We find a good agreement between the absorption energies observed experimentally here and density functional theory calculations reported earlier.

© 2019 Optical Society of America under the terms of the [OSA Open Access Publishing Agreement](#)

## 1. Introduction

Organic light emitting diodes (OLED) based on metal chelates such as tris(8-hydroxyquinoline) aluminum, Alq<sub>3</sub>, have been widely studied for several decades since Tang and VanSlyke demonstrated light emission from the first practical electroluminescent device based on a double-organic-layer structure of Alq<sub>3</sub> and a diamine film in the late 80's [1]. Despite the widespread use of Alq<sub>3</sub>, there has been a broad search for new materials with improved properties, in particular, with respect to their chemical and electrochemical stability [2–8].

Materials based on tetravalent silicon using a Si(ligand)<sub>2</sub> design have emerged as a material class, which could provide the sought after improved stability, low molecular weights, and low dipole moments. We have recently reported on the successful synthesis of a neutral, hexacoordinate silicon-based fluorescent complex Si(bzimpy)<sub>2</sub> [9]. Our results indicate that Si(bzimpy)<sub>2</sub> exhibits inherent advantages such as the tunability of the luminescence in the visible spectrum, greater thermal stability, and a high charge mobility that is comparable to that of Alq<sub>3</sub>. In addition to the successful material synthesis, we have fabricated simple, functional OLED structures consisting exclusively of Si(bzimpy)<sub>2</sub> sandwiched between ITO and Al films which showed a yellow-green emission at  $\lambda = 560$  nm [9].

Further advances in the design and fabrication of Si(bzimpy)<sub>2</sub>-based OLED structures require the accurate knowledge of the optical properties of this material. Although optical absorption, fluorescent excitation and emission behavior have been studied, the complex dielectric function of Si(bzimpy)<sub>2</sub> has not been reported yet.

In this paper, we report on the determination of the complex dielectric function of  $\text{Si}(\text{bzimpy})_2$  in the spectral range from 0.65 eV to 4.1 eV (300 nm to 1900 nm) using spectroscopic ellipsometry. Optical model calculations using a model dielectric function for the  $\text{Si}(\text{bzimpy})_2$  thin film which is composed of a sum of oscillators with Gaussian and Tauc-Lorentz broadening were able to accurately reproduce the experimental ellipsometry data. The absorption energies identified here are found to be in good agreement with results from our time-dependent density functional theory (TD-DFT) calculations and absorption measurements reported earlier [9].

## 2. Experiment

### 2.1. Sample preparation

$\text{Si}(\text{bzimpy})_2$  was synthesized by adding  $\text{SiCl}_4$  to a chloroform solution containing two equivalents of the bzimpy ligand, 2,6-bis(benzimidazol-2'-yl)pyridine, and four equivalents of triethylamine. A thin-film sample with a nominal thickness of 100 nm was fabricated by thermal deposition of the synthesized  $\text{Si}(\text{bzimpy})_2$  on a Si substrate at a pressure of  $10^{-6}$  mbar. The deposition rate was adjusted to 0.5-0.8 Å/s using a commercial deposition system (MB-EVAP) with an integrated deposition controller (SQC-310C). In order to achieve a homogeneous film thickness across the sample, a rotating substrate holder was employed during the deposition. The rotational speed was 15 rpm throughout the thin film growth. Further details regarding the deposition system are omitted here for brevity and the interested reader is referred to Ref. [9], which includes a comprehensive description of the  $\text{Si}(\text{bzimpy})_2$  synthesis and the deposition of thin  $\text{Si}(\text{bzimpy})_2$  films using thermal evaporation. Complementary atomic force microscopy (AFM) characterization was performed on the investigated sample indicating a root mean square roughness  $R_{\text{rms}} = 2.09$  nm and a mean roughness of 1.6 nm. These surface properties are very similar to those in our previous publication Ref. [9]. In addition, X-ray diffraction (XRD) measurements were carried out in order to confirm that the  $\text{Si}(\text{bzimpy})_2$  sample investigated here is amorphous.

After the deposition, the  $\text{Si}(\text{bzimpy})_2$  thin-film sample was investigated using a commercial spectroscopic ellipsometer (V-VASE, J.A. Woollam Company Inc.). The ellipsometer is equipped with a HS-190 scanning monochromator and uses a Si and an InGaAs photodiode as detectors to allow continuous coverage of the spectral range from 0.65 eV to 4.1 eV. The instrument operates in a classical rotating polarizer - sample - rotating analyzer configuration and has an adjustable compensator [10,11]. We obtained  $\Psi$ - and  $\Delta$ -spectra at room temperature in the near infrared, visible, and ultraviolet spectral range with a resolution of 0.05 eV at three different angles of incidence ( $65^\circ$ ,  $70^\circ$ , and  $75^\circ$ ).

### 2.2. Data acquisition and analysis

The experimental  $\Psi$ - and  $\Delta$ -data were analyzed using stratified-layer optical model calculations with a commercial ellipsometry data analysis software package (WVASE32, J.A. Woollam Co.). The optical model required to accurately reproduce the experimental response is composed of three layers including a Si substrate, a  $\text{SiO}_2$  layer, and a  $\text{Si}(\text{bzimpy})_2$  layer. Accounting for the surface roughness of the  $\text{Si}(\text{bzimpy})_2$  thin film was found to provide only an insignificant improvement of the match between the experimental and the best-model calculated ellipsometric spectra and was therefore omitted in the applied optical model. Ellipsometric data obtained from the Si substrate prior to the  $\text{Si}(\text{bzimpy})_2$  thin film deposition was used to determine the thickness of the native  $\text{SiO}_2$  layer. The native  $\text{SiO}_2$  layer thickness was not further varied during the analysis of the ellipsometric data obtained from the  $\text{Si}(\text{bzimpy})_2$  sample. Standard model dielectric functions were used to account for the optical response of the Si substrate and the  $\text{SiO}_2$  layer [12].

The accurate representation of the experimental ellipsometry data shown in Figs. 1 and 2 required a parameterized model dielectric function for  $\text{Si}(\text{bzimpy})_2$  which allowed the reproduction

of the optical signatures of the band-gap and higher order electronic transitions. Analyzing spectroscopic ellipsometry data including such features in the ultraviolet, visible, and near-infrared region requires mathematical dispersion functions which maintain Kramers-Kronig consistency while providing sufficient flexibility to reproduce the experimental lineshape adequately. Dielectric function models composed of mixed oscillators with Gaussian and Tauc-Lorentz broadening have been demonstrated to allow this [13]. For the Si(bzimp)<sub>2</sub> sample investigated here, the mixed oscillator model results in a better fit of the experimental  $\Psi$  and  $\Delta$  data throughout the investigated spectral range when compared to a dielectric function model based entirely on oscillators with Lorentz and Tauc-Lorentz broadening, as was used in our previous work [9]. Thus, the parameterized model dielectric function used here to describe the optical response of Si(bzimp)<sub>2</sub> in the experimentally accessible spectral range is composed of a combination of an oscillator with Tauc-Lorentz broadening and a set of two oscillators with Gaussian broadening [13]:

$$\begin{aligned} \varepsilon(E) &= \varepsilon_1(E) + i\varepsilon_2(E), \\ &= 1 + \frac{A}{E_0^2 - E^2} + \sum_{i=1}^2 \text{Gau}(E, A, E_0, \Gamma) + \\ &\quad \text{TL}(E, A, E_0, \Gamma, E_g), \end{aligned} \quad (1)$$

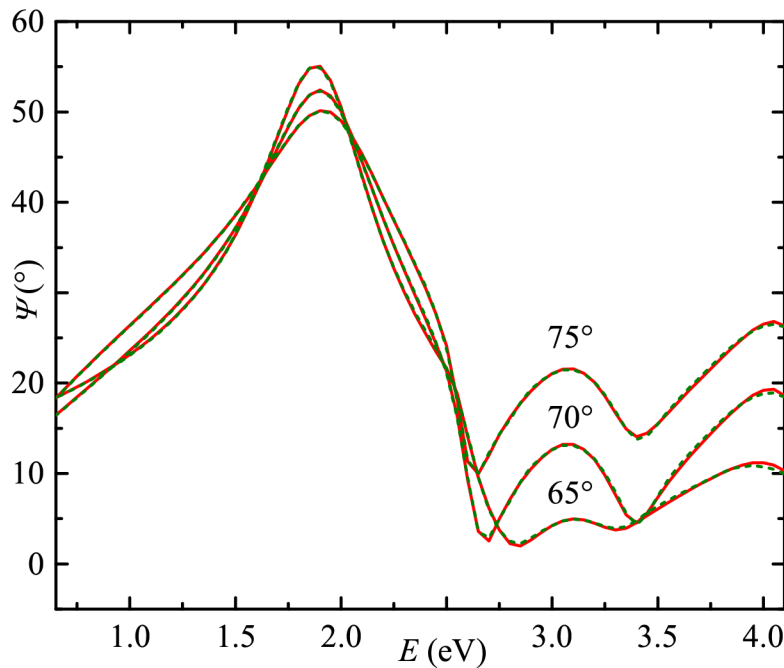


**Fig. 1.** Experimental (green dashed line) and best-model (red solid line)  $\Psi$ -spectra for the Si(bzimp)<sub>2</sub> sample measured at three different angles of incidence  $\Phi_a = 65^\circ, 70^\circ,$  and  $75^\circ$  in spectral range from 0.65 eV to 4.1 eV.

where  $\varepsilon_1(E)$  and  $\varepsilon_2(E)$  denote the real and imaginary parts of the complex dielectric function, respectively. The functions  $\text{TL}(E, A, E_0, \Gamma, E_g)$  and  $\text{Gau}(E, A, E_0, \Gamma)$  represent the oscillators with Tauc-Lorentz and Gaussian broadening, which account for the contribution of the electronic band gap and higher order electronic transitions, respectively. Herein, the physical relevant parameters  $A, E_0, \Gamma,$  and  $E_g$  indicate the oscillator amplitude, resonant energy, broadening and band gap energy, respectively. Higher energy contributions to the dielectric function cause

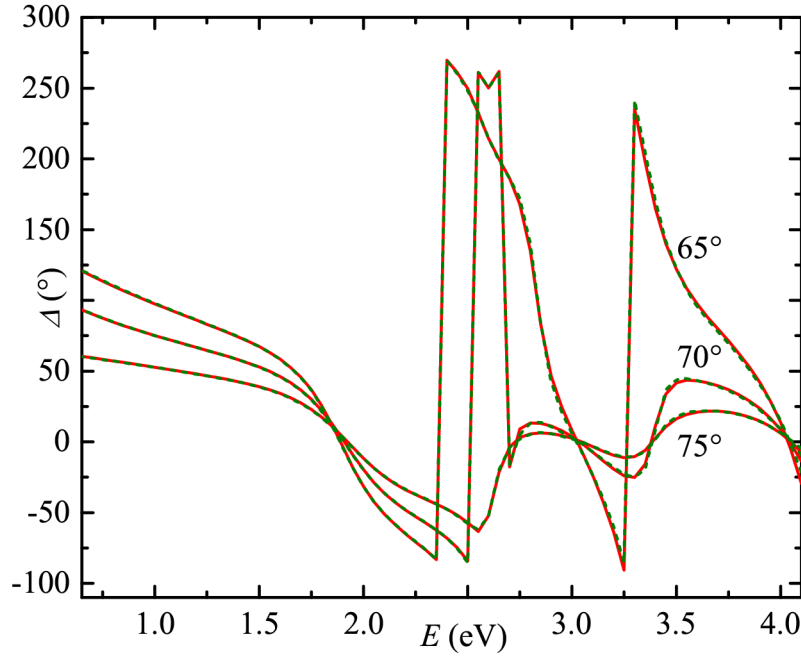


**Fig. 2.** Same as Fig. 1 but for the  $\Delta$ -spectra obtained for the  $\text{Si}(\text{bzimpy})_2$  sample at three different angles of incidence.

absorptions outside of the measured spectral range, which contribute to the dispersion of  $\varepsilon_1(E)$ . These contributions are included in the model by a pole, i.e., a Lorentz oscillator with vanishing broadening  $A/(E_0^2 - E^2)$ .

In particular the pole which is used to describe the dispersion of the real part of the dielectric function  $\varepsilon_1$  due to absorptions occurring outside of the measured spectral range is now addressed specifically.

The imaginary part of  $\text{TL}(E, A, E_0, \Gamma, E_g)$  and  $\text{Gau}(E, A, E_0, \Gamma)$  is given by  $\varepsilon_2^{\text{TL}}$  and  $\varepsilon_2^{\text{Gau}}$ , respectively [13–15]:

$$\varepsilon_2^{\text{TL}}(E) = \begin{cases} \frac{AE_0\Gamma(E-E_g)^2}{(E^2-E_0^2)^2+\Gamma^2E^2} \cdot \frac{1}{E} & E > E_g \\ 0 & E \leq E_g \end{cases}, \quad (2)$$

$$\varepsilon_2^{\text{Gau}}(E) = Ae^{-\left(\frac{E-E_0}{f\Gamma}\right)^2} - Ae^{-\left(\frac{E+E_0}{f\Gamma}\right)^2}, \quad (3)$$

where the constant  $f = 1/2\sqrt{\ln(2)}$  in Eqn. (3) defines the full width at half maximum of broadening denoted by  $\Gamma$ . The real part of the complex dielectric function  $\varepsilon_1(\omega)$  is determined by Kramers-Kronig transformation of  $\varepsilon_2^{\text{Gau}}$  and  $\varepsilon_2^{\text{TL}}$  as part of the data analysis [13].

During the data analysis, relevant model parameters ( $A$ ,  $E_0$ ,  $\Gamma$ ,  $E_g$ , and layer thickness  $t$  of the  $\text{Si}(\text{bzimpy})_2$  thin film) were varied using a Levenberg-Marquardt-based algorithm until a best match between experimental and calculated data was achieved, which is shown in Figs. 1 and 2, discussed below. The best-model dielectric function of  $\text{Si}(\text{bzimpy})_2$  is shown in Fig. 3.

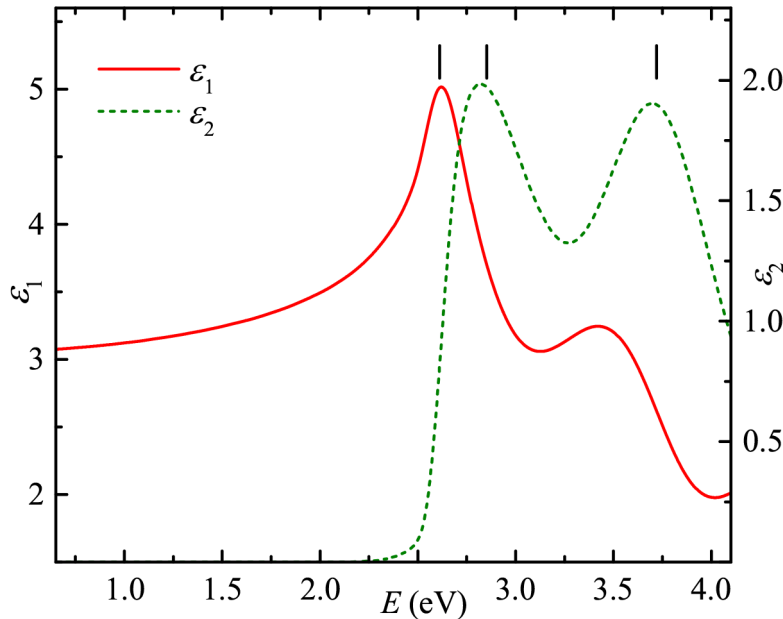


**Fig. 3.** Real  $\varepsilon_1$  (solid red line) and imaginary  $\varepsilon_2$  part (dotted green line) of the model dielectric function given in Eqn. (1) using the best-fit model parameters summarized in Table 1. The transition energies for the Tauc-Lorentz and the Gaussian oscillators are indicated as vertical lines.

**Table 1.** Summary of the best-model parameters obtained for the dielectric function of  $\text{Si}(\text{bzimpy})_2$  during the optical model analysis. The error limits correspond to 90% confidence limits.

Oscil.	A	$E_0$ (eV)	$\Gamma$ (eV)	$E_g$ (eV)
Pole	$(94 \pm 5) \text{ eV}^2$	$8.2 \pm 0.2$	—	—
Gau <sub>1</sub>	$1.12 \pm 0.05$	$3.73 \pm 0.01$	$0.56 \pm 0.03$	—
Gau <sub>2</sub>	$0.40 \pm 0.06$	$2.86 \pm 0.03$	$0.47 \pm 0.02$	—
TL	$(132 \pm 13) \text{ eV}$	$2.60 \pm 0.01$	$0.30 \pm 0.02$	$2.51 \pm 0.01$

### 3. Results and discussion

Figures 1 and 2 show the experimental (green dashed line) and best-model calculated (red solid line)  $\Psi$ - and  $\Delta$ -spectra for of the  $\text{Si}(\text{bzimpy})_2$  thin film sample measured at room temperature, respectively. The experimental data was acquired at three different angles of incidence ( $65^\circ$ ,  $70^\circ$ , and  $75^\circ$ ). An excellent agreement between the experimental and best-model calculated data can be observed over the entire spectral range.

The spectrum of  $\Psi$  shown in the Fig. 1 is dominated by a Fabry-Pérot oscillation in the range from 0.61 eV to 2.5 eV where the  $\text{Si}(\text{bzimpy})_2$  film is transparent. The structures in the spectral range from 2.5 eV to 4.1 eV are due to the band gap at  $E_g = (2.51 \pm 0.01) \text{ eV}$  and higher order electronic transitions at 2.86 eV and 3.73 eV. The behavior observed in the ellipsometric data corroborates our previous spectrophotometer-based absorption measurements in the ultraviolet to visible spectral range of  $\text{Si}(\text{bzimpy})_2$  in solution [9].

The best-model transition energies, amplitudes, and broadening parameters of the  $\text{Si}(\text{bzimpy})_2$  model dielectric function are summarized in Table 1. A thickness of the  $\text{Si}(\text{bzimpy})_2$  thin film  $t = 98.6 \pm 0.1 \text{ nm}$  is determined, which corresponds well with the nominal thickness for this sample.

Figure 3 depicts the real and imaginary part of the best-fit model dielectric function for the Si(bzimpy)<sub>2</sub> thin film in the spectral range from 0.65 eV to 4.1 eV. Si(bzimpy)<sub>2</sub> is transparent below the band gap in the spectral range from 0.65 eV to 2.5 eV. The spectral range above 2.5 eV is dominated by two strong absorption bands at 3.73 eV and 2.86 eV, which are described by two oscillators with Gaussian broadening.

A good agreement is found between the oscillator energies determined with this mixed oscillator model and the transition energies we have identified using TD-DFT calculations [9]. In accordance with these earlier observations, we find here that the amplitude of the transition at 3.73 eV is larger than the amplitude of the transition observed at 2.86 eV (see Table 1). In addition, the absorption onset marked by the Tauc-Lorentz band gap energy of 2.51 eV is well reproduced. The Tauc-Lorentz energy  $E_0$  corresponds to transitions identified at approximately 2.69 eV in the TD-DFT calculations.

#### 4. Conclusion

A recently synthesized fluorescent organic complex Si(bzimpy)<sub>2</sub> has been characterized for the first time using spectroscopic ellipsometry. We report on a mixed oscillator model dielectric function composed of Gaussian and Tauc-Lorentz oscillators, which allows the identification of electronic transitions including quantitative values for physically meaningful oscillator parameters. This model dielectric function allows the accurate description of the ellipsometric data obtained from a Si(bzimpy)<sub>2</sub> thin film sample in spectral range from 0.65 eV to 4.1 eV at multiple angles of incidence. A good agreement between the observed transition energies and TD-DFT results reported earlier is found [9]. The complex dielectric function of Si(bzimpy)<sub>2</sub> reported here fills a critical gap in the knowledge of a new class of materials based on tetravalent silicon using a Si(ligand)<sub>2</sub> design, which has emerged recently. In addition, our model establishes the accurate optical dispersion of Si(bzimpy)<sub>2</sub> which provides further insights into important optical features of Si(bzimpy)<sub>2</sub>-based optoelectronic devices such as energy dissipation and phase variation. Numerical simulations of such devices will substantially benefit from the precisely determined dielectric function.

#### Funding

NSF within the I/UCRC Center for Metamaterials (1624572); NSF | MPS | Division of Chemistry (CHE) (CHE-1800331); Swedish Agency for Innovation Systems (2014-04712); NanoSURE program (CHE-1460867).

#### Acknowledgments

The authors are grateful for support from the National Science Foundation (1624572) within the I/UCRC Center for Metamaterials, the NSF Division of Chemistry (CHE-1800331), the Swedish Agency for Innovation Systems (2014-04712), and Department of Physics and Optical Science of the University of North Carolina at Charlotte. In addition, the authors acknowledge support from the UNC Charlotte Targeted Research Internal Seed Program and support for M.K. through a graduate student career preparedness supplement to the NSF-REU/DOD-ASSURE supported NanoSURE program (CHE-1460867).

#### References

1. C. W. Tang and S. A. VanSlyke, "Organic electroluminescent diodes," *Appl. Phys. Lett.* **51**(12), 913–915 (1987).
2. X. Zhou, M. Pfeiffer, J. Blochwitz, A. Werner, A. Nollau, T. Fritz, and K. Leo, "Very-low-operating-voltage organic light-emitting diodes using a *p*-doped amorphous hole injection layer," *Appl. Phys. Lett.* **78**(4), 410–412 (2001).
3. V. A. Montes, R. Pohl, J. Shinar, and P. Anzenbacher Jr, "Effective manipulation of the electronic effects and its influence on the emission of 5-substituted tris(8-quinolinolate) aluminum (III) complexes," *Chem. - Eur. J.* **12**(17), 4523–4535 (2006).

4. V. M. Manninen, W. A. Omar, J. P. Heiskanen, H. J. Lemmetyinen, and O. E. Hormi, "Synthesis and characterization of tris-(5-amino-8-hydroxyquinoline) aluminum complexes and their use as anode buffer layers in inverted organic solar cells," *J. Mater. Chem.* **22**(43), 22971–22982 (2012).
5. S.-H. Liao, J.-R. Shiu, S.-W. Liu, S.-J. Yeh, Y.-H. Chen, C.-T. Chen, T. J. Chow, and C.-I. Wu, "Hydroxynaphthridine-derived group III metal chelates: wide band gap and deep blue analogues of green Alq<sub>3</sub> (tris(8-hydroxyquinolate)aluminum) and their versatile applications for organic light-emitting diodes," *J. Am. Chem. Soc.* **131**(2), 763–777 (2009).
6. P. K. Nayak, N. Agarwal, F. Ali, M. P. Patankar, K. Narasimhan, and N. Periasamy, "Blue and white light electroluminescence in a multilayer oled using a new aluminium complex," *J. Chem. Sci.* **122**(6), 847–855 (2010).
7. W. A. Omar, H. Haverinen, and O. E. Hormi, "New Alq<sub>3</sub> derivatives with efficient photoluminescence and electroluminescence properties for organic light-emitting diodes," *Tetrahedron* **65**(47), 9707–9712 (2009).
8. C. Pérez-Bolívar, S.-Y. Takizawa, G. Nishimura, V. A. Montes, and P. Anzenbacher Jr, "High-efficiency tris(8-hydroxyquinoline)aluminum (Alq<sub>3</sub>) complexes for organic white-light-emitting diodes and solid-state lighting," *Chem. - Eur. J.* **17**(33), 9076–9082 (2011).
9. M. Kocherga, J. Castaneda, M. G. Walter, Y. Zhang, N.-A. Saleh, L. Wang, D. S. Jones, J. W. Merkert, B. Donovan-Merkert, Y. Li, T. Hofmann, and T. A. Schmedake, "Si (bzimpy)<sub>2</sub>—a hexacoordinate silicon pincer complex for electron transport and electroluminescence," *Chem. Commun.* **54**(100), 14073–14076 (2018).
10. B. Johs, J. A. Woollam, C. M. Herzinger, J. N. Hilfiker, R. A. Synowicki, and C. L. Bungay, "Overview of variable-angle spectroscopic ellipsometry (VASE): II. advanced applications," *Proc. SPIE* **10294**, 1029404 (1999).
11. H. Fujiwara, *Spectroscopic Ellipsometry Principles and Applications* (John Wiley & Sons Inc., Hoboken, NJ 07030, USA, 2007).
12. C. Herzinger, B. Johs, W. McGahan, J. A. Woollam, and W. Paulson, "Ellipsometric determination of optical constants for silicon and thermally grown silicon dioxide via a multi-sample, multi-wavelength, multi-angle investigation," *J. Appl. Phys.* **83**(6), 3323–3336 (1998).
13. R. Synowicki and T. E. Tiwald, "Optical properties of bulk c-ZrO<sub>2</sub>, c-MgO and a-As<sub>2</sub>S<sub>3</sub> determined by variable angle spectroscopic ellipsometry," *Thin Solid Films* **455-456**, 248–255 (2004).
14. G. Jellison Jr. and F. Modine, "Parameterization of the optical functions of amorphous materials in the interband region," *Appl. Phys. Lett.* **69**(3), 371–373 (1996).
15. G. Jellison Jr. and F. Modine, "Erratum: "parameterization of the optical functions of amorphous materials in the interband region"[*Appl. Phys. Lett.* 69, 371 (1996)]," *Appl. Phys. Lett.* **69**(14), 2137 (1996).